Low-Order GAM Admire System in Landing Preparation Phase[1]

Ionel IORGA

*Corresponding author
University of Craiova
Alexandru Ioan Cuza Str. 13, 200585 Craiova, Romania
ionel.iorga@yahoo.com

DOI: 10.13111/2066-8201.2011.3.3.8

Abstract: *In this paper the symbolic and numeric computations for the simplified GAM (Generic Aerodynamic Model) Admire system are presented . The numeric computations were performed into the MatLab environment with the aim of presenting to the reader the details of the preparation for landing of the airplane generic model. Regarding the symbolic computations that have been made it's worth to mention here the fact that they concerned the issues of stability in the manner that the trim point for the low order non-linear system was computed and an analysis of the eigenvalues of the Jacobian matrix associated to the system, which has been evaluated in the trim point, was performed. The case of the stable longitudinal level descending flight and the case of transition to a state appropriate for the touch-down are presented. It is shown the fact that the plane can regain stability if the real moment for touch-down is missed by reentering into the stable longitudinal level descending flight (by usage of the control* δe*).*

Key Words: *generic aerodynamic model, Admire longitudinal system, oscillations, stability.*

1. INTRODUCTION

The Generic Aerodynamic Model is a theoretical model of a small fighter aircraft with a delta-canard configuration which was developed by Saab AB, as a basis for their simulations and used, for research, by the Aeronautical Research Institute of Sweden in order to construct a complete small fighter single-seated delta-canard model (Admire).

A detailed mathematical and explicit description of the two models (Admire being, in fact, a version of the GAM) are not given but the available data's are presented in the form of schematic pictures (see, for example Figure 1) and data table. Also suggestions for the GAM aircraft mass and the mass distribution can be found in [2] and a good reference for GAM Admire is [3]. The original GAM Admire system has twelve states [3], but for the simplicity of the analysis low order non-linear explicit differential models can be used [4], [1], [5], in order to cite just a few papers.

One more reason to study with a more detailed attention the phenomena that can occur in the phase of landing is the possibility of a Pilot Induced Oscillations (PIO) event occurrence. The PIO always has a trigger event and that may be a sudden change in the direction and in the speed of the wind or due to the negative effect of nonlinearities induced, for example, by the actuators. Indeed, many of these PIO's, often with catastrophic consequences, appear in the landing phase. For a more detailed exposition on the PIO events, the reader can consult [6], [7], for example.

[1] The research has been partly supported by the Project CNCSIS ID-95 of the Council for Scientific Research of the Higher Education of Romania

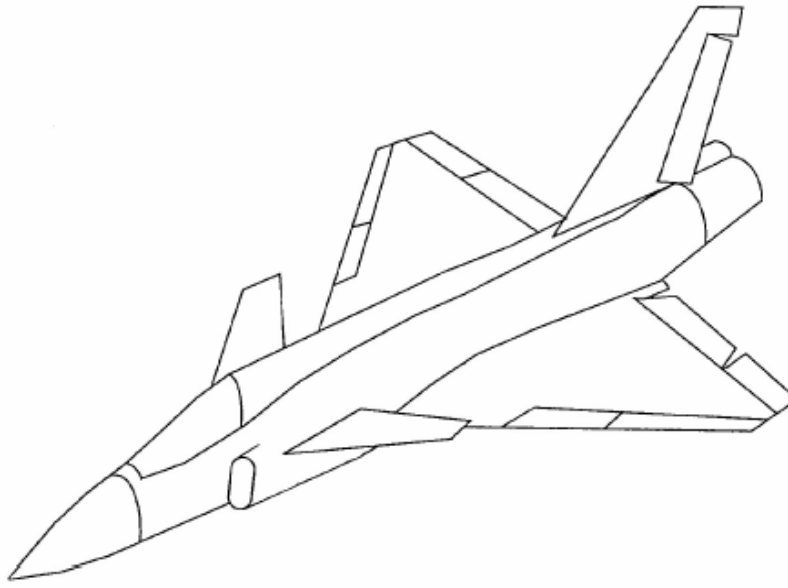

Figure 1: The GAM Admire generic figure (pp. 8 from [3])

2. THE SIMPLIFIED LONGITUDINAL GAM ADMIRE SYSTEM

From [1] the following system, with constant speed, is considered:

$$\begin{cases} \dot{\alpha} = z_\alpha \alpha + z_{\delta_e} \delta e + \dfrac{g}{V_0} \cos(\theta) + q \\ \dot{q} = \overline{m}_\alpha \alpha + \overline{m}_q q + \overline{m}_{\delta_e} \delta e + \dfrac{g}{V_0} (m_{\dot{\alpha}} \cos(\theta) - \overline{a} \sin(\theta)) - \dfrac{1}{a} \alpha q \\ \dot{\theta} = q \end{cases} \tag{1}$$

for which the numeric values (2) apply:

$$\begin{cases} g = 9.81 \dfrac{m}{s^2};\ V_0 = 84.5 \dfrac{m}{s};\ a = -.2424;\ \overline{a} = 1.424 \\ z_\alpha = -.7986;\ z_{\delta_e} = -.2603;\ \overline{m}_{\delta_e} = -8.2668 \\ \overline{m}_\alpha = -6.5315;\ \overline{m}_q = -.6957;\ m_{\dot{\alpha}} = -.162 \end{cases} \tag{2}$$

For the system (1) the state system is $X = (\alpha, q, \theta)$, in which:

- α is the incidence angle
- θ represents the pitch angle
- $q = \dot{\theta}$ (the variation of θ)

and the input vector U has one dimension for the mentioned simplified vector, $U = (\delta_e)$, in which δ_e represents the angle of the elevon.

2.1. COMPUTING THE TRIM POINTS

For computing the trim points for the system (1) it is important to notice the fact that there is no explicit restriction for the input $\overline{\delta}e$, so, in function of $\overline{\delta}e$ the trim point can change.

In the following a complementary way of computing the bounds of $\overline{\delta}e$, regarding the stability of the system, relative to the method presented in [1], is used. The following method, applied in this case is original regarding this problem and, compared to the one in [1] is sligthly different.

From the system (1) it can be noticed the fact that $\overline{q} = 0$, so the following results:

$$\begin{cases} z_\alpha \overline{\alpha} + z_{\delta_e} \overline{\delta}e + \dfrac{g}{V_0} \cos(\overline{\theta}) = 0 \\ \overline{m}_\alpha \overline{\alpha} + \overline{m}_{\delta_e} \overline{\delta}e + \dfrac{g}{V_0} (m_{\dot{\alpha}} \cos(\overline{\theta}) - \overline{a} \sin(\overline{\theta})) = 0 \end{cases} \tag{3}$$

Following the steps from [1], from the first equation, the expression for $cos(\overline{\theta})$ (4) is obtained:

$$cos(\overline{\theta}) = -\frac{V_0}{g} (z_\alpha \overline{\alpha} + z_{\delta_e} \overline{\delta}e) \tag{4}$$

Relation (4) is relaced into the second equation of the system (3) obtaining $\sin(\overline{\theta})$:

$$\sin(\overline{\theta}) = \frac{V_0}{g\overline{a}} [\overline{m}_\alpha \overline{\alpha} + \overline{m}_{\delta_e} \overline{\delta}e \ - m_{\dot{\alpha}} (z_\alpha \overline{\alpha} + z_{\delta_e} \overline{\delta}e \ )] \tag{5}$$

From (4) and (5) it follows that

$$\overline{\alpha}^2 k_1 + 2\overline{\alpha}\overline{\delta}e \ k_2 + \overline{\delta}e \ ^2 k3 - (\frac{g}{V_0})^2 = 0 \tag{6}$$

in which the following notations were made:

$$\begin{cases} k_1 = (\dfrac{1}{\overline{a}})^2 (\overline{m}_\alpha - m_{\dot{\alpha}} z_\alpha)^2 + z_\alpha^2 \\ k_2 = (\dfrac{1}{\overline{a}})^2 (\overline{m}_\alpha - m_{\dot{\alpha}} z_\alpha)(\overline{m}_{\delta_e} - m_{\dot{\alpha}} z_{\delta_e}) + z_\alpha z_{\delta_e} \\ k3 = (\dfrac{1}{\overline{a}})^2 (\overline{m}_{\delta_e} - m_{\dot{\alpha}} z_{\delta_e})^2 + z_{\delta_e}^2 \end{cases} \tag{7}$$

For the relation (7) the discriminant $\Delta_{\overline{\alpha}}$ is computed, on which the following positivity condition is putted:

$$\overline{\delta}_e^{\,2} (k_2^2 - k_1 k_3) + k_1 (\frac{g}{V_0})^2 = 0 \tag{8}$$

Resolving the equation (8) the follwing interval results:

$$\overline{\delta}_e \in (-.160042, \cdots, .160042) \tag{9}$$

The result (9) is similar to the one from [1] with slight differences given by the numeric approximation of the coefficients.

In the following the manner of computing the trim points $\overline{X}$ is shown.

From the first equation of the system (3) the following relation is obtained:

$$\overline{\alpha} = -\frac{1}{z_\alpha}\left(\frac{g}{V_0}cos(\overline{\theta}) + z_{\delta_e}\overline{\delta}e\right) \tag{10}$$

(10) is replaced in the second equation of the system (3) resulting the following:

$$q_1 cos(\overline{\theta}) + q_2 sin(\overline{\theta}) + q_3\overline{\delta}e = 0 \tag{11}$$

were the following notations have been made:

$$\begin{cases} q_1 = \dfrac{g}{V_0}(m_{\dot{\alpha}} - \dfrac{\overline{m}_\alpha}{z_\alpha}) \\ q_2 = -\overline{a}\dfrac{g}{V_0}sin(\overline{\theta}) \\ q_3 = \overline{m}_{\delta_e} - z_{\delta_e}\dfrac{\overline{m}_\alpha}{z_\alpha}) \end{cases} \tag{12}$$

From (11), by noting $y = cos(\overline{\theta})$ and squaring it results:

$$y^2(q_1^2 + q_2^2) + 2yq_1\overline{\delta}_e q_3 + \overline{\delta}_e{}^2 q_3^2 - q_2^2 = 0 \tag{13}$$

Solving the algebraic equation (13) and taking into account the relation (9) then for $\overline{\theta}$, Figure 2 results.

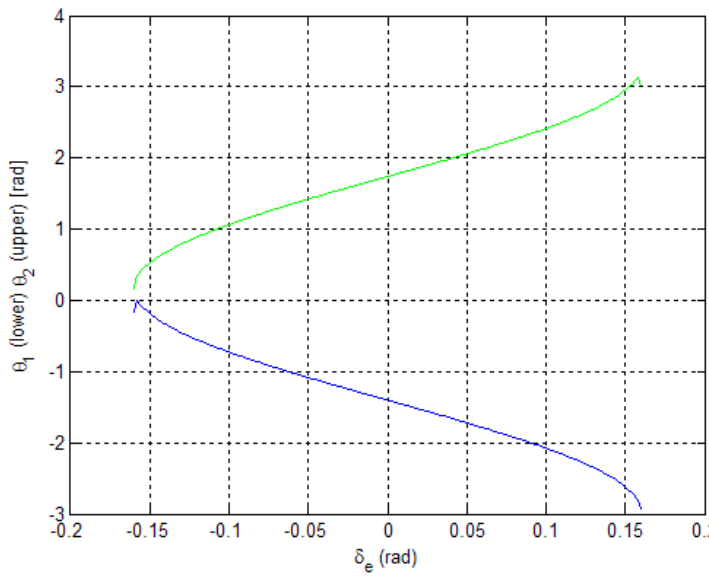

Figure 2: The graphic of the $\overline{\theta}$, depending on the input δ_e, for the system (1)

Tacking into account the equation (11) Figure 3 is obtained.

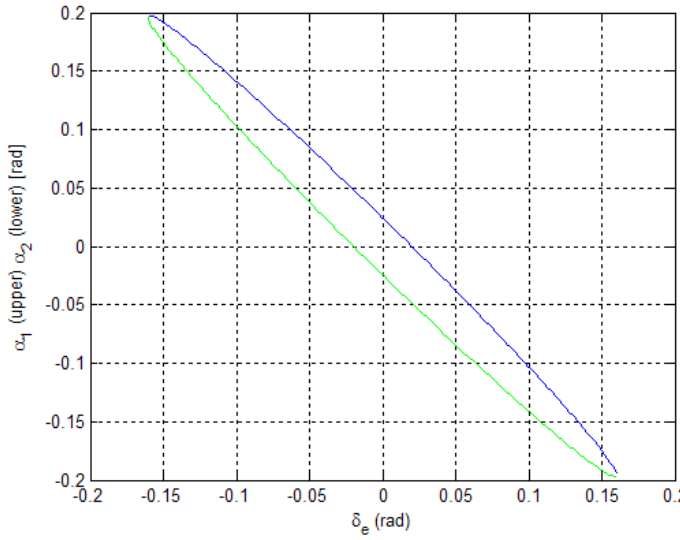

Figure 3: The graphic of the $\overline{\alpha}$, depending on the input δ_e , for the system (1)

Figures 2 and 3 match with the ones from [1]. For the range of $\overline{\delta}_e$ the following sets appear :

- $\overline{X}_1 = (\overline{\alpha}_1, 0, \overline{\theta}_1)$
- $\overline{X}_2 = (\overline{\alpha}_2, 0, \overline{\theta}_2)$

2.2 THE STABILITY OF THE LINEARISED SYSTEM

By considering the maximum of the roots real parts of the Jacobian matrixes characteristic polynomials, evaluated in points (3), associated to the system (1), it can be deduced that for the set $\overline{X}_1$ the linearised system is stable (see the Figure 4).

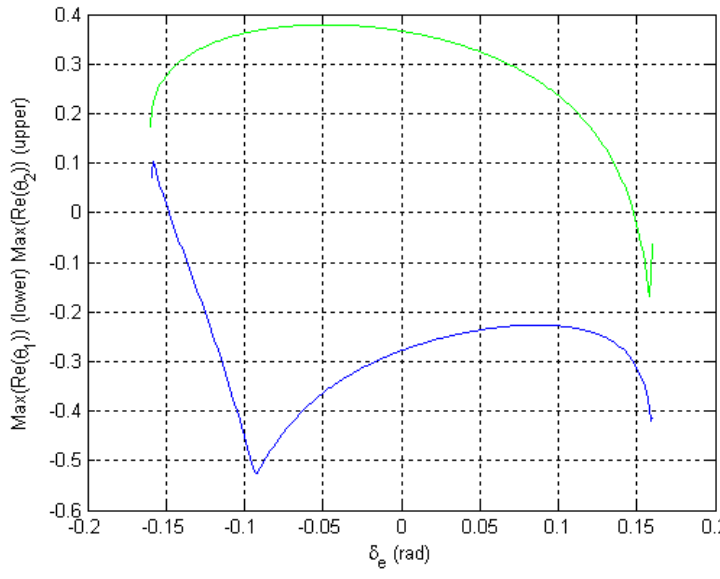

Figure 4: The graphic of the maximum of the roots real parts of the Jacobian matrixes characteristic polynomials

2.3. MATLAB SIMULATIONS FOR THE LOW-ORDER NONLINEAR MODEL

For the following two subsections the general scheme of the simulink low-order nonlinear model is given in the Figure 5. For all the cases, the airplane scheme is given in Figure 6 and the subsystems α and q are represented in Figures 7 and 8, respectively.

The model plane is used in a stable descending, longitudinal flight.

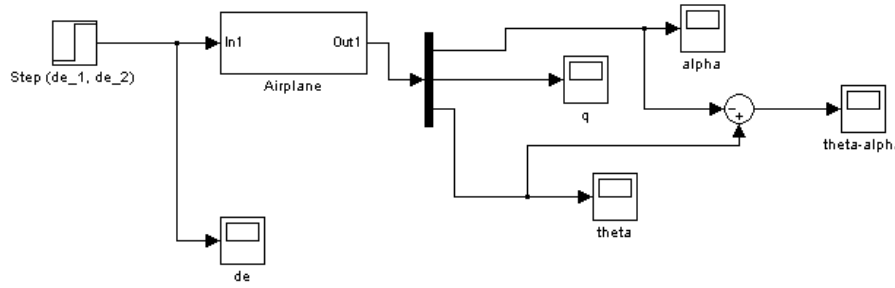

Figure 5: The scheme of the simulink low-order nonlinear model

Observation 2.1. *In Figure 5 we notice the presence of the step input block. This block plays an important role for the evolution of the system (1) from one equilibrium state into the other. These states are initiated by* δ_{01} *and* δ_{02}*, repectively, and they can be by identified as points in Figures 2 and 3.*

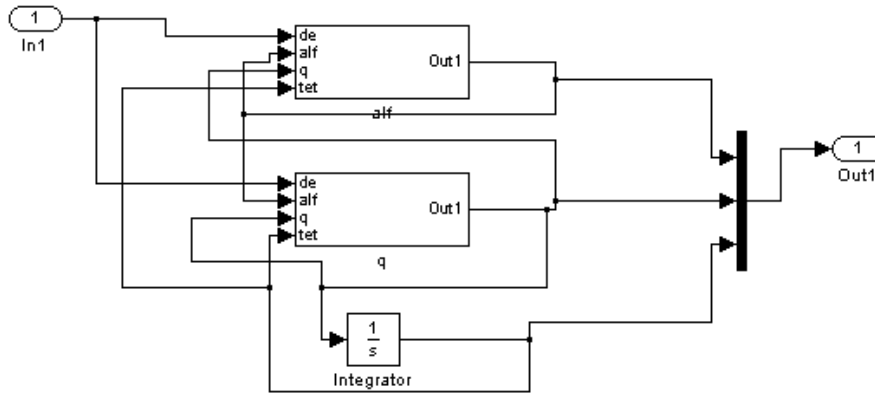

Figure 6: The graphical representation of the airplane scheme

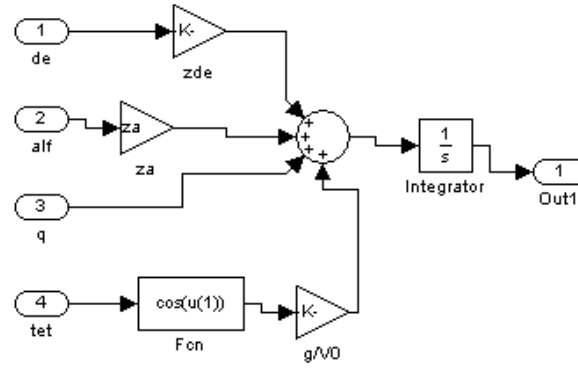

Figure 7: The graphical representation of the subsystem α

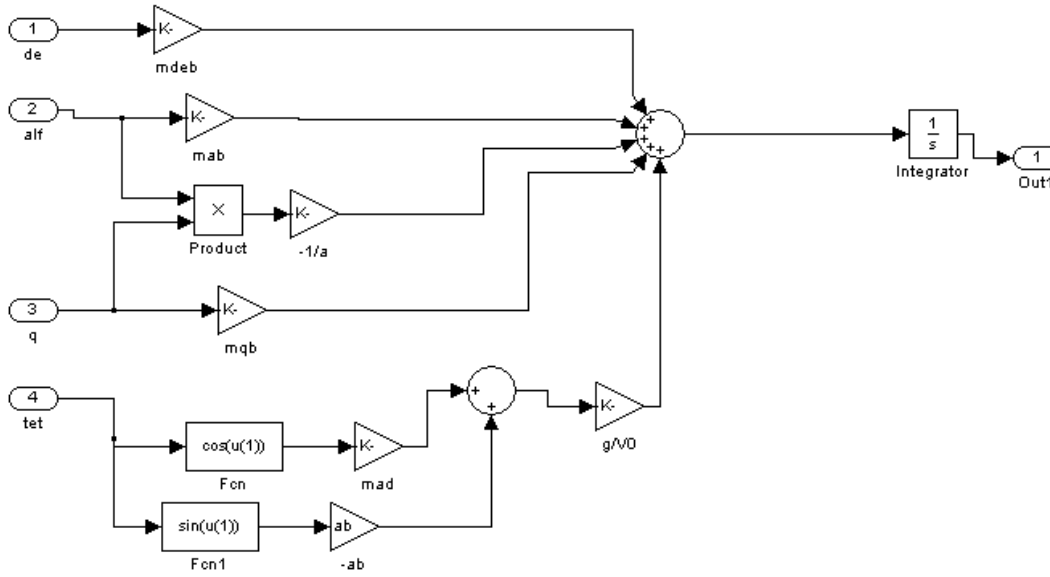

Figure 8: The graphical representation of the subsystem *q*

2.3.1 Simulation for $\delta_0 = -0.1578$

In this case $\delta_{01} = \delta_{02} = \delta_0 = -0.1578$.

From (11) and (15) $\Rightarrow$ $\overline{X} = \{0.1968, 0, -0.0015\}$.

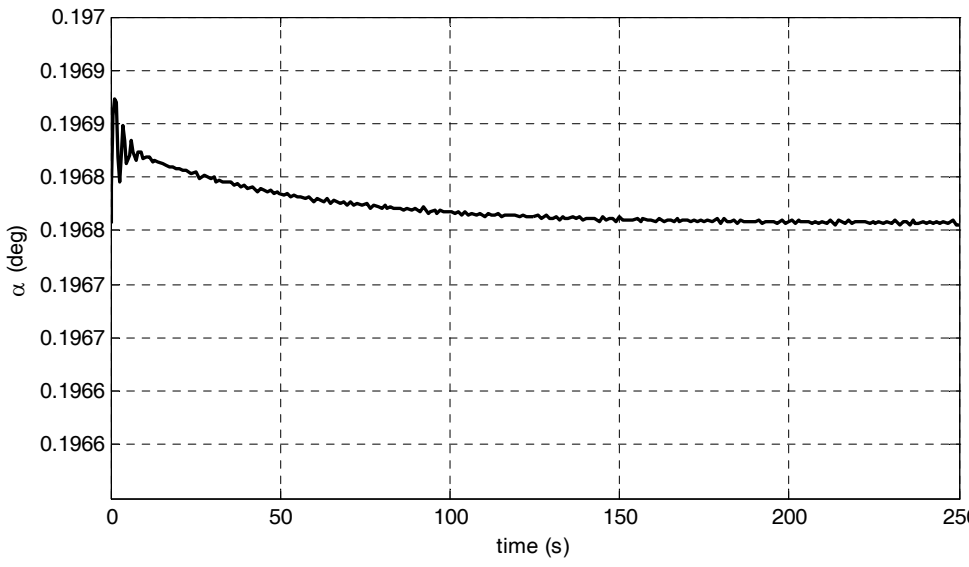

Figure 9: The graphical representation of the angle α for $\delta_0 = -0.1578$

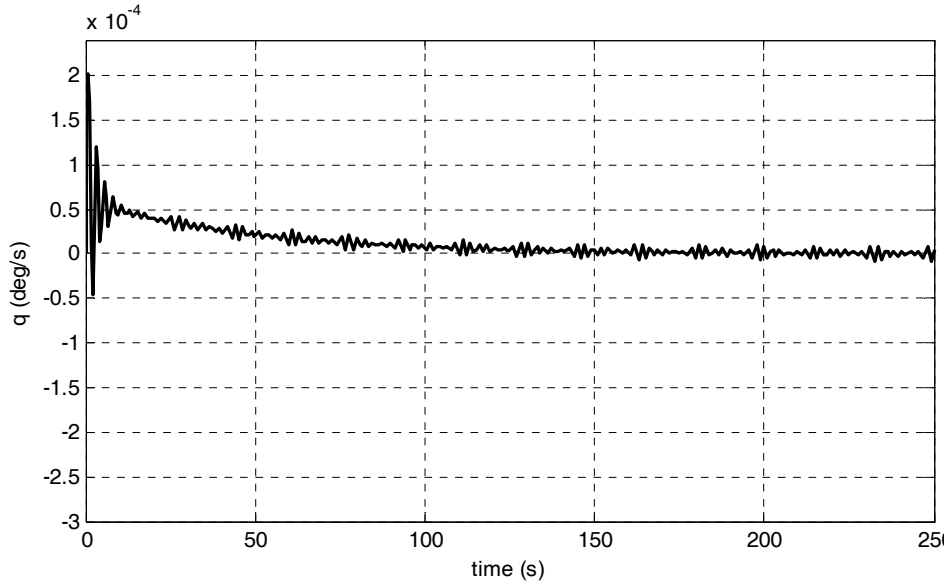

Figure 10: The graphical representation of the variation q for $\delta_0 = -0.1578$

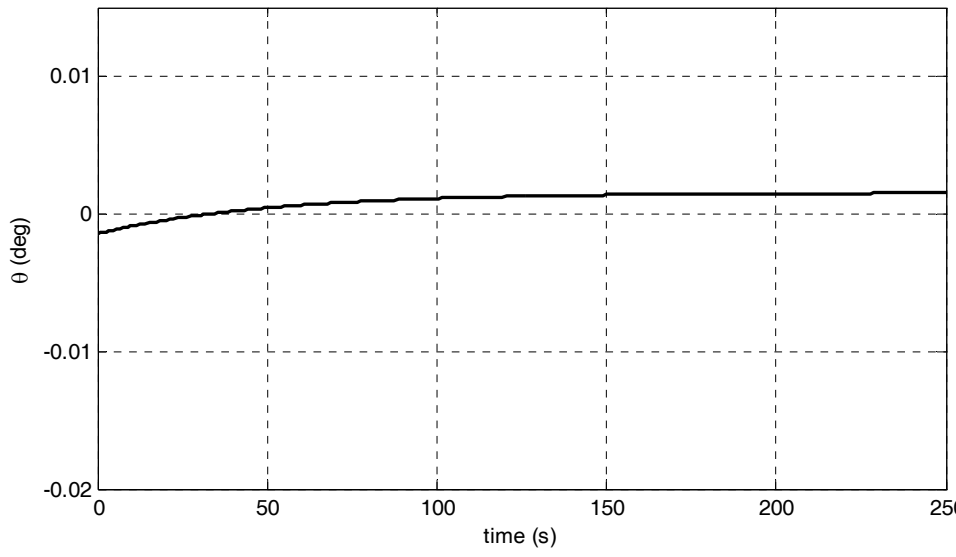

Figure 11: The graphical representation of the angle θ for $\delta_0 = -0.1578$

Observation 2.2. *This is a typical case of stable descending longitudinal flight equilibrium.*

$$\begin{cases} \theta = 0 \\ \theta - \alpha < 0 \end{cases}$$

Observation 2.3. *For example, for* $\delta_0 = 0$, θ *has a high negative value and this fact confirms numerically as well, the supplementary restriction on* δ_e *(18) input given in pp.278 from [1].*

$$\delta_e \in (-.1582703;-.061270] \cup [.1087296;.154729)$$

2.3.2 Simulation for $\delta_{01} = -0.1578$ and $\delta_{02} = -0.167$

In this case, we have $\delta_{01} = -.1578$ and $\delta_{02} = -0.167$.

From (11) and (15) $\Rightarrow$ $\overline{X} = \{0.1968, 0, -0.0015\}$.

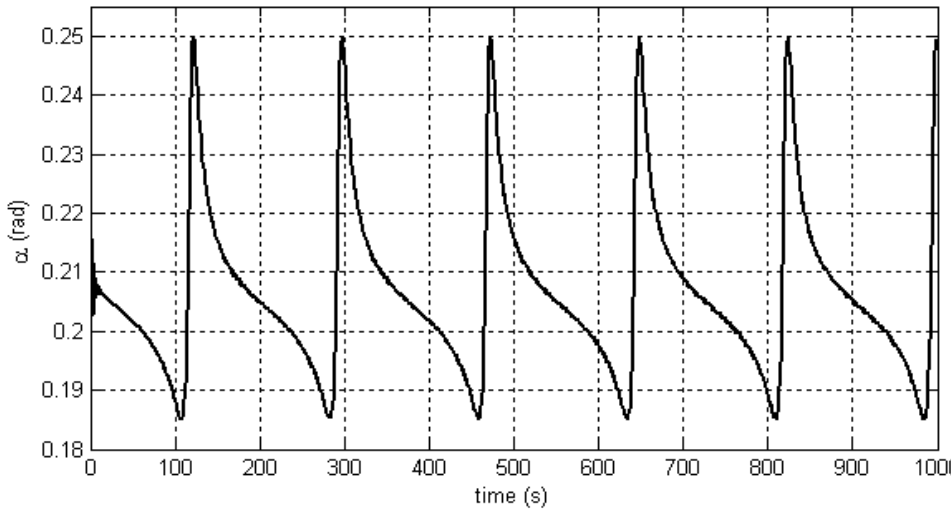

Figure 12: The graphical representation of the angle α for $\delta_{01} = -.1578$ and $\delta_{02} = -0.167$

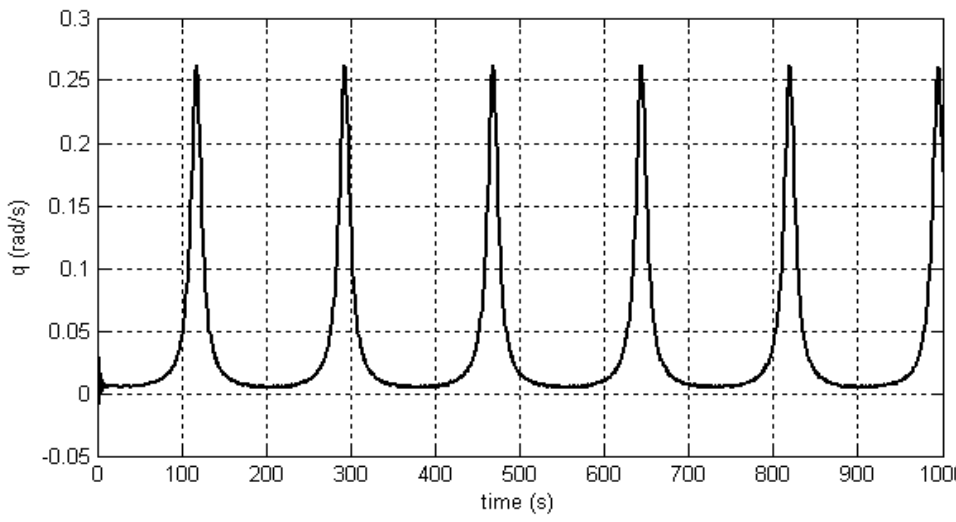

Figure 13: The graphical representation of the variation q for $\delta_{01} = -.1578$ and $\delta_{02} = -0.167$

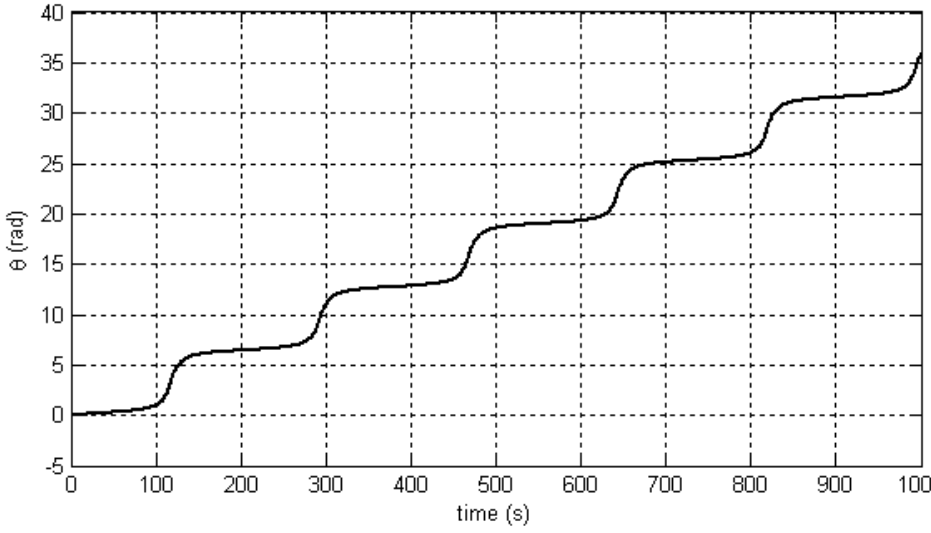

Figure 14: The graphical representation of the angle θ for $\delta_{01} = -.1578$ and $\delta_{02} = -0.167$

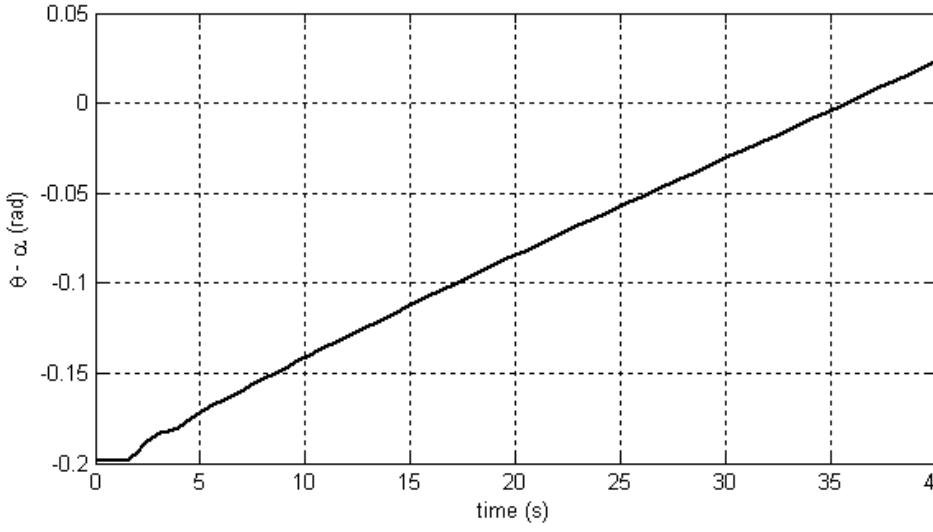

Figure 15: The graphical representation of the angle $\theta - \alpha$ for $\delta_{01} = -.1578$ and $\delta_{02} = -0.167$

Observation 2.4 *This case expresses the transfer from a stable longitudinal flight equilibrium to an appropiate touch-down state (19). Figure 15 shows that the touch-down can be correctly performed in about 35 sec, otherwise, after that time, if the control is not reset to its original value, the system can enter in oscillations. In pp. 279 from [1], is stated that this behavior "is a saddle node bifurcation phenomenon and from the mathematical point of-view is non-catastrophic" (the control δe can be reset).*

$$\begin{cases} \theta \approx 0.2 \\ \theta - \alpha = 0 \end{cases}$$

3. CONCLUSIONS

In the subsection 2.3.2, for the low-order GAM Admire system behavior in the landing preparation phase we can conclude that if the real touch-down is greater than the pre-computed one then the landing may be catastrophic (θ oscillates and increases) (Figure 15). However if the control δe is reset to its original value the system reenters into stable longitudinal level descending flight (please see the Figure 16). For the future work the usage of the robustness, with incertitudes, would provide a more realistic approach to these simuation (a good reference for this is, for example,

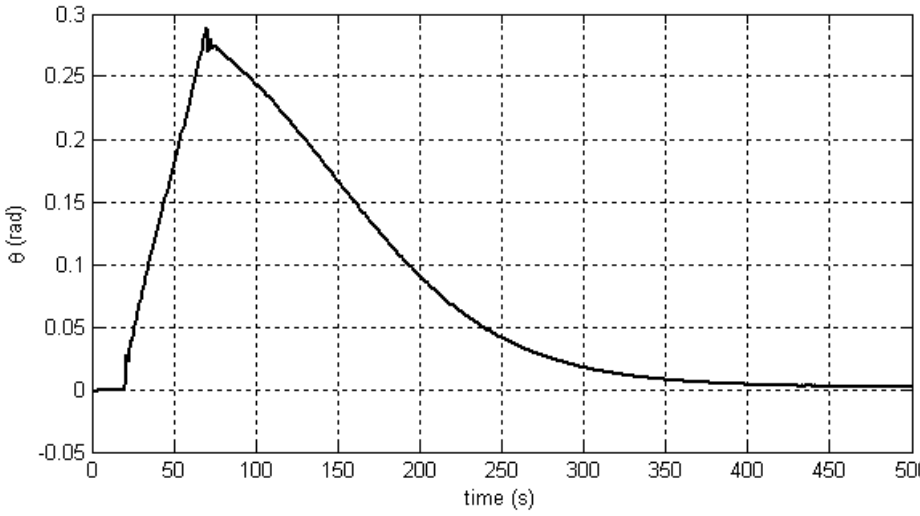

Figure 16: The graphical representation of the angle θ for $\delta_{01} = -.1578$ and $\delta_{02} = -0.167 \;\; for \;\; t \in (20,70) \;\; s$

REFERENCES

[1] A. Ionita, A.M. Balint and St. Balint, *Limit Cycle Behaviour in Aircraft Longitudinal Terminal Phase*, Seventh International Conference on Mathematical Problems in Engineering, Aerospace and Sciences, Genova, 2008.

[2] H. Backstrőm, *Report on the usage of the Generic Aerodata Model*, Technical Report. AAB Aircraft AB, SAAB Military Aircraft, S-58199 Linkping Sweden, May 1997.

[3] L. Forssel and U. Nilsson, *ADMIRE The Aero-Data Model In a Research Environment,* Version 4.0, Model Description, Report FOI-R--1624--SE ISSN-1650-1942, December 2005.

[4] A. M. Balint, St. Balint and A. Ionita, *Oscillation Susceptibility Analysis of the ADMIRE Aircraft along the Path of Longitudinal Flight Equilibriums in Two Different Mathematical Models*, Hindawi Publishing Corporation Diferential Equations and Nonlinear Mechanics Volume 2009, Article ID 842656, 26 pages doi:10.1155/2009/842656

[5] St. Balint et al., *Oscillation susceptibility analysis along the path of longitudinal flight equilibriums,*Nonlinear Analysis (2008), Nonlinear Analysis: Theory, Methods & Applications, In Press, 2008, available on-line doi:1010.16/j.na.2008.10.054

[6] R. A. Hess, *Unified Theory for Aircraft Handling Qualities and adverse Aircraft-Pilot Coupling*, Journal of Guidance, Control and Dynamics, Vol. **20** No 6, pp. 1141-1148, 1997.

[7] D. Klyde et al, *Unified Pilot-Induced Oscillation Theory, Volume 1: PIO Analysis with Linear and Nonlinear Effective Vehicle Characteristics, Including Rate. s.l.: Air Force Research Laboratories*, Wright-Patterson AFB, WL-TR-96-3028, 1995.

[8] J-F. Magni, S. Bennani, J. Terluw, *Robust flight control. A design challenge*, Springer-Verlag, London , 1997.